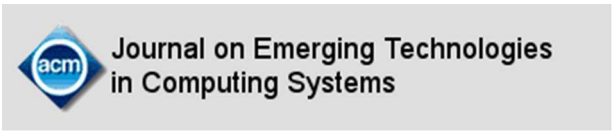

A Learning-Based Thermal-Sensitive Power Optimization Approach for Optical NoC

Journal:	*Journal on Emerging Technologies in Computing Systems*
Manuscript ID	Draft
Manuscript Type:	SI: Silicon Photonics
Date Submitted by the Author:	n/a
Complete List of Authors:	Zhang, Zhe; Shanghai Jiao Tong University, Department of Micro/Nano Electronics Ye, Yaoyao; Shanghai Jiao Tong University, Department of Micro/Nano Electronics
Computing Classification Systems:	

A Learning-Based Thermal-Sensitive Power Optimization Approach for Optical NoCs

Zhe Zhang, Yaoyao Ye
Department of Micro/Nano Electronics
Shanghai Jiao Tong University, Shanghai, China

Optical networks-on-chip (NoCs) based on silicon photonics have been proposed as emerging on-chip communication architectures for chip multiprocessors with large core counts. However, due to thermal sensitivity of optical devices used in optical NoCs, on-chip temperature variations cause significant thermal-induced optical power loss which would counteract the power advantages of optical NoCs. To tackle this problem, in this work, we propose a learning-based thermal-sensitive power optimization approach for mesh or torus-based optical NoCs in presence of temperature variations. The key techniques proposed includes an initial device setting and thermal tuning mechanism which is a device-level optimization technique, and a learning-based thermal-sensitive adaptive routing algorithm which is a network-level optimization technique. Simulation results of an 8x8 mesh-based optical NoC show that the proposed initial device setting and thermal tuning mechanism confines the worst-case thermal-induced energy consumption to be on the order of tens of pJ/bit, by avoiding significant thermal-induced optical power loss caused by temperature-dependent wavelength shifts. Besides, it shows that the learning-based thermal-sensitive adaptive routing algorithm is able to find an optimal path with the minimum estimated thermal-induced power consumption for each communication pair. The proposed routing has a greater space for optimization especially for applications with more long-distance traffic.

Categories and Subject Descriptors: C.1.2 [**Processor Architectures**]: Multiple data stream architectures (Multiprocessors)—*interconnection architectures*; *parallel processors*

General Terms: Design, Performance, Power consumption

Additional Key Words and Phrases: Chip multiprocessor, optical network-on-chip, optical-electronic router

1. INTRODUCTION

By enabling energy-efficient parallel processing in lower clock frequencies, chip multiprocessors have become a natural platform for embedded systems and high-performance computing. State-of-the-art chip multiprocessor systems consist of tens of or even hundreds of processor cores on a chip. Networks-on-chip (NoCs) have been widely proposed for on-chip communication in more than a decade, which scale better than on-chip shared bus and ad-hoc network when the number of cores increases [Dally and Towles 2001; Benini and De Micheli 2002]. However, due to the limitations of electronic interconnects in power efficiency and bandwidth density, as well as issues of high-frequency crosstalk noise and parasitic capacitance, there are still bandwidth, power efficiency and reliability bottlenecks in traditional NoCs based on electronic interconnects.

As compared to electronic interconnect, silicon photonics based optical interconnect can enable significantly increased bandwidth density, low power consumption and low latency. Optical NoCs based on silicon photonic devices such as silicon microresonator (MR) and optical waveguide, offer a new solution to addressing the on-chip communication issues [Shacham et al. 2007; Vantrease et al. 2008; Pan et al. 2009; Mo et al. 2010; Ye et al. 2013; Ramini et al. 2014; Werner et al. 2015; Faralli et al. 2016]. Considering the high efficiency of electronic interconnect in local com-

munication as well as in control, optical NoCs are often controlled and configured in electronic domain. Three-dimensional integration technologies provide the support for realization of mixed-technology electronic-controlled optical NoCs. Shacham *et al.* proposed a circuit-switched augmented-torus optical NoC based on a blocking 4x4 optical switch [Shacham et al. 2007]. Crossbar-based optical on-chip network architectures were proposed for high throughput at the cost of a large amount of silicon photonic devices [Vantrease et al. 2008; Pan et al. 2009]. Mo *et al.* proposed a hierarchical mesh-based optical NoC, which uses electronic wormhole switching for local traffic and circuit switching in the global optical network [Mo et al. 2010]. Ye *et al.* proposed a 3D mesh-based optical NoC, which takes advantages of 3D topology to improve network performance [Ye et al. 2013]. Werner *et al.* proposed an all-optical mesh-like design with a contention-free routing algorithm [Werner et al. 2015]. Based on the wavelength-selective switching function of MR, several 5x5 optical routers have been designed for mesh or torus-based optical NoCs [Gu et al. 2009; Xie et al. 2010; Poon et al. 2009; Ji et al. 2011]. For example, Cygnus is a low-power non-blocking 5x5 optical router which uses 16 MRs [Gu et al. 2009].

However, due to the thermo-optic effect in silicon photonics, one critical challenge is the thermal sensitivity of optical NoCs, which may counteract their advantages in power efficiency as compared with their electronic counterpart [Dokania and Apsel 2009]. Due to uneven power density on chip and limited thermal conductivity of packaging materials, chip temperature fluctuates temporally as well as spatially. The on-chip temperature can vary by more than 30^oC across a steady-state chip under typical operating conditions [Skadron et al. 2004]. As a result of thermo-optic effect, wavelength-selective silicon photonic devices such as MRs, which are widely used in optical NoCs, suffer from temperature-dependent wavelength shifts [Padgaonkar and Arbor 2004]. An investigation of thermal issues of optical NoCs shows that, the thermal related wavelength mismatch between the laser located in the source node and the switching elements in intermediate nodes on path may cause excessive optical power loss, and thus significant thermal-induced power consumption [Ye et al. 2012].

In order to tackle the thermal problems, device-level thermal compensation techniques such as thermal tuning and low-temperature-dependence MRs have been proposed to compensate for the temperature-dependent wavelength shift of MRs [Gan et al. 2007; Lee et al. 2007]. Besides, system-level thermal modeling and thermal-aware designs based on signal-to-noise ratio (SNR) analysis have been proposed to overcome the thermal challenges in optical NoCs [Ye et al. 2012; Ye et al. 2014; Li et al. 2015a]. Adaptive routing which takes account of on-chip temperature variations is another way to improve the reliability of optical NoCs in presence of temperature variations [Xiang et al. 2013; Guo et al. 2015; Li et al. 2015b; Yang and Ampadu 2016].

Q-learning based adaptive routing algorithms take advantages of Q-learning technique to optimize the routing decisions according to runtime network state [Farahnakian et al. 2011; Ebrahimi et al. 2012; Feng et al. 2010]. Several adaptive routing algorithms based on Q-learning have been proposed for electronic NoCs. In work [Farahnakian et al. 2011; Ebrahimi et al. 2012], a Q-learning based adaptive routing was proposed to reduce the latency in traditional electronic NoCs. In

work [Feng et al. 2010], a hierarchical Q-learning based deflection routing algorithm was proposed for a mesh-based electronic NoC to improve the performance in presence of faults.

In this work, we propose a learning-based thermal-sensitive power optimization approach for mesh or torus-based optical NoCs in presence of on-chip temperature variations, which takes advantages of the Q-learning technique for optimization purpose. The proposed power optimization approach includes both device-level optimization and network-level routing optimization. To avoid significant optical power loss caused by the temperature-dependent wavelength shift in optical switching elements, an initial device setting is proposed to ensure that thermal tuning can be applied to compensate for the wavelength mismatch between the laser source and the optical switching elements in a path. On the basis of the initial device setting and thermal tuning mechanism, a learning-based thermal-sensitive adaptive routing algorithm is proposed to further optimize the thermal-induced power consumption by making routing decisions taking account of temperature variations. The odd-even turn model is used to find feasible shortest and deadlock-free paths for learning, and the Q-learning technique is used to optimize the path selection with the objective of minimizing estimated thermal-induced power consumption for packet transmission.

The rest of paper is organized as follows. Section 2 reviews the related works. Section 3 introduces the modeling of thermal effects in optical NoCs. In Section 4, we propose the initial device setting and thermal tuning mechanism. In Section 5, we detail the learning-based thermal-sensitive adaptive routing algorithm. Section 6 presents simulation results and comparisons in terms of thermal-induced energy efficiency and network performance. Last, Section 7 concludes.

2. RELATED WORKS

Previous works have investigated the thermal sensitivity of photonic devices used in optical NoCs. The temperature-dependent wavelength shift in silicon MR is found to be about $50 - 100pm/K$, which is non-negligible in practical use [Baehr-Jones et al. 2005; Padgaonkar and Arbor 2004; Dumon et al. 2006]. Besides, investigations of the temperature sensitivity of VCSELs (vertical cavity surface emitting laser) show that their temperature-dependent wavelength shift is comparable to or even larger than that of silicon MRs [Michalzik and Ebeling ; Mogg et al. 2004]. Further more, because of the mutual shift between lasing wavelength and peak material gain wavelength under temperature variations, VCSEL power efficiency degrades seriously at high temperatures [Syrbu et al. 2008]. There are also investigations of the temperature-dependent behaviors of Ge-based photodetectors. It is found that the detection sensitivity does not change obviously at high temperatures [Koester et al. 2006; Morse et al. 2006].

Some device-level thermal compensation techniques have been proposed to compensate for the temperature-dependent wavelength shift for siliocn MRs. Thermal tuning by local microheaters is an alternative solution, and the tuning efficiency is on the order of several mW/nm [Gan et al. 2007; Geng et al. 2009]. However, it is relatively slow and power inefficient [Gan et al. 2007; Geng et al. 2009]. Another possible solution is to fabricate silicon MRs with low temperature dependence

by passive compensation techniques. Low-temperature-dependence MRs and even athermal MRs have been demonstrated by applying proper polymer materials as upper cladding [Lee et al. 2007; Raghunathan et al. 2010]. However, there are still compatibility issues when fabricating athermal MRs with CMOS technology.

Besides, some efforts have been made to overcome the thermal challenges in optical NoCs from system-level perspectives. Run-time thermal management techniques such as workload migration and dynamic voltage and frequency scaling (DVFS) were proposed to reduce the on-chip temperature gradients [Li et al. 2010; Zhang et al. 2014]. Due to the limitations of these thermal management techniques, device-level thermal compensation techniques are still in need. In work [Ye et al. 2012], authors systematically modeled thermal effects in optical NoCs and proposed several low-temperature-sensitivity techniques. In work [Li et al. 2015a], authors proposed a thermal-aware methodology to design optical NoCs with distributed CMOS-compatible VCSELs, based on steady-state thermal simulations and signal-to-noise ratio (SNR) analysis.

Adaptive routings have been adopted in optical NoC designs, which can dynamically make routing decisions according to runtime network conditions. A fault-tolerant and deadlock-free routing algorithm was proposed to improve the reliability of optical NoCs by taking account of the actual bandwidth of optical links affected by temperature fluctuations as well as manufacturing errors [Xiang et al. 2013]. A fault-tolerant node-reuse adaptive routing algorithm was proposed to tolerate arbitrary number of faults from MRs in optical NoCs, which improves the packet delay and SNR [Guo et al. 2015]. In work [Li et al. 2015b], a thermally resilient optical NoC architecture design was proposed to support reliable and low bit error rate (BER) on-chip communications in presence of large temperature variations. In order to improve the BER, a fault-tolerant routing was proposed to route packets away from hot regions, and through cooler regions, to their destinations. In work [Yang and Ampadu 2016], a thermal-aware fault-tolerant routing mechanism that exploits path diversity was proposed to perform adaptive routing in a hybrid optical-electronic NoC in presence of on-chip thermal variations. In work [Asadi et al. 2016], a turning model routing was proposed to find paths with the lowest optical power loss. Q-learning based adaptive routing algorithms have been proposed for traditional electronic NoCs, taking advantages of Q-learning technique to optimize routing decisions according to runtime network state. In work [Farahnakian et al. 2011; Ebrahimi et al. 2012], a Q-learning based adaptive routing was proposed to reduce the latency in traditional electronic NoCs. In work [Feng et al. 2010], a hierarchical Q-learning based deflection routing algorithm was proposed for a mesh-based electronic NoC to improve the performance in presence of faults.

In this work, we propose a learning-based thermal-sensitive power optimization approach for mesh or torus-based optical NoCs in presence of temperature variations. The proposed power optimization approach includes both device-level optimization and network-level routing optimization. The proposed key techniques include an initial device setting and thermal tuning mechanism, and a learning-based thermal-sensitive adaptive routing algorithm to further optimize the thermal-induced power consumption.

3. THERMAL EFFECTS IN OPTICAL NOCS

In this section, we briefly introduce the thermal effects in photonic devices including silicon MR and VCSEL that are widely used in optical NoCs. The thermal modelings described in this section serve as the basis for the thermal-sensitive power optimization techniques proposed in this work.

3.1 Thermo-optic effect

As a result of thermo-optic effect, silicon refractive index is temperature dependent and follows Equation (1), where n_0 is the silicon refractive index at room temperature, dn/dT is the thermo-optic coefficient of silicon, and ΔT is the change of temperature. Physical measurements show that the thermo-optic coefficient dn/dT of silicon is on the order of $10^{-4}/K$ and is nonlinear over a large temperature range at 1550nm wavelength [Della Corte et al. 2000].

$$n = n_0 + \frac{dn}{dT}\Delta T \tag{1}$$

3.2 Temperature sensitivity of VCSEL

VCSEL is a good candidate for on-chip laser source because of the low power consumption, high modulation bandwidth, and manufacturing advantages which provide an opportunity for better integration. It has been chosen to be used as on-chip laser source by many optical NoC architectures in order to fully integrate optical NoCs on chip. Investigations show that both the lasing wavelength and output power of VCSEL are sensitive to ambient temperature [Michalzik and Ebeling ; Mogg et al. 2004]. As shown in Equation (2), the lasing wavelength of a VCSEL (λ_{VCSEL}) red-shifts approximately linearly with the ambient temperature T_{VCSEL}, where λ_{VCSEL_0} is its lasing wavelength at room temperature T_0, and ρ_{VCSEL} is defined as its temperature-dependent wavelength shift coefficient.

$$\lambda_{VCSEL} = \lambda_{VCSEL\_0} + \rho_{VCSEL}(T_{VCSEL} - T_0) \tag{2}$$

Besides, the output power of a VCSEL degrades at higher temperatures. Assuming that the VCSEL is driven by current I, its output optical power P_{TX} follows Equation (3), where α is the minimum threshold current, T_{th} is the temperature at which the threshold current is the minimum, β is a coefficient related to the temperature dependance of the threshold current, ε is the slope efficiency at 0^oC, and γ is a positive coefficient [Chen et al. 2006]. For the VCSEL demonstrated in [Syrbu et al. 2008], when the temperature changes from room temperature to 80^oC, the slope efficiency decreases from $0.36mW/mA$ to $0.23mW/mA$, and the maximum emission power decreases from $4mW$ to $1.5mW$ correspondingly.

$$P_{TX} = (I - \alpha - \beta(T_{VCSEL} - T_{th})^2)(\varepsilon - \gamma \cdot T_{VCSEL}) \tag{3}$$

3.3 Temperature sensitivity of silicon MR

Silicon MR has been widely used as a wavelength-selective basic optical switching element in optical NoCs. The switching functionality a ring-based MR can be illustrated by a simplified model shown in Figure 1. When the MR is turned on by applying a voltage, the resonant wavelength matches with the input optical signal. The input optical signal would be switched to the drop port, and we define this as

an active switching. When the MR is turned off, the resonant wavelength shifts away from the input optical signal wavelength. Thus the input optical signal will be directed to the through port, and we define this as a passive switching.

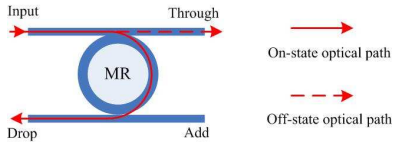

Fig. 1. The switching functionality of a MR

Due to the thermo-optic effect, the resonant wavelength of a silicon MR (λ_{MR}) is sensitive to ambient temperature, which follows Equation (4), where λ_{MR_0} is its resonant wavelength at room temperature T_0, ρ_{MR} is the temperature-dependent wavelength shift coefficient, and T_{MR} is the ambient temperature. Both theoretical analysis and experiment results have confirmed a linear relationship between the wavelength shift and the ambient temperature.

$$\lambda_{MR} = \lambda_{MR\_0} + \rho_{MR}(T_{MR} - T_0) \tag{4}$$

Temperature variations across a chip will result in wavelength mismatches between the optical signal emitted by laser located in the source node and the resonant wavelength of intermediate switching elements in path. The thermal-induced optical power loss (in dB) inserted by an active switching follows Equation (5), where 2δ is the 3-dB bandwidth of the basic optical switching element, κ^2 is the fraction of power coupling between the waveguide and the ring, and κ_p^2 is the power loss per round-trip of the ring [Xiao et al. 2007]. When $2\kappa^2 \gg \kappa_p^2$, nearly full power transfer can be achieved at the peak resonance, exhibiting a low insertion loss. A deviation from the peak resonant wavelength would result in more power loss in an active switching especially if with a narrow 3-dB bandwidth. For a basic optical switching element working at the 1550nm wavelength range, if the quality factor is on the order of 10^4, a 10^oC temperature change would make the power spectrum shift about *0.5nm* and result in a power loss variation of about *16dB* for optical signals carried by 1550nm wavelength.

$$L_{AS} = 10log((\frac{2\kappa^2 + \kappa_p^2}{2\kappa^2})^2 \cdot (1 + (\lambda_{VCSEL} - \lambda_{MR})^2/\delta^2)) \tag{5}$$

4. AN INITIAL DEVICE SETTING AND THERMAL-TUNING MECHANISM

In this section, we first get the modeling of the thermal-induced optical power loss in optical NoC caused by temperature-dependent wavelength shifts in laser source and optical switching elements. Considering that thermal tuning can only red-shift the MR wavelength by heating, we then propose an initial device setting condition to avoid significant thermal-induced optical power loss and thermal tuning power consumption.

4.1 Thermal-induced optical power loss and energy consumption

For an optical path consisting of N_1 active switching stages and N_2 passive switching stages, we can get the thermal model in Equation (6), where P_{TX} is the output power of the laser source (Equation (3)), L_{AS_i} is the thermal-induced optical power loss inserted in the i_{th} active switching stage, L_{PS_j} is the thermal-induced optical power loss inserted in the j_{th} passive switching stage, L_{WG} is the waveguide propagation loss in the optical path, S_{RX} is the receiver sensitivity. The thermal model shows that under a high power loss in the optical path caused by chip temperature fluctuations, more input power would be needed by the transmitter to guarantee enough optical power reaching the receiver.

$$P_{TX} - \sum_{i=1}^{N_1} L_{AS_i} - \sum_{j=1}^{N_2} L_{PS_j} - L_{WG} \geq S_{RX} \tag{6}$$

The thermal-induced power consumption for packet transmission in an optical NoC in presence of temperature variations involves the power consumed for payload transmission in optical domain (P_{opti}), and the power consumed for control purpose in electronic domain (P_{elec}). The power consumed in optical domain is thermal sensitive, including the power consumed by optical/electronic (O/E) interfaces ($P_{O/E}$), and the power consumed for thermal tuning (P_{tuning}).

$$P = P_{opti} + P_{elec} \tag{7}$$

$$P_{opti} = P_{O/E} + P_{tuning} \tag{8}$$

A typical O/E interface includes serializer, driver, VCSEL laser source, photodetector, TIA-LA circuits and deserializer. Table I shows the energy consumption of each component in O/E interface. Here we use the serializer and deserializer design in [Poulton et al. 2007], and the VCSEL driver and TIA-LA designs in [Kromer et al. 2005]. With certain device technologies, power dissipated in an O/E interface is mainly governed by the laser source. In order to compensate for the thermal-induced optical power loss, the laser driving current I should be large enough to satisfy the condition shown in Equation (6). The range of optical power loss decides the VCSEL power consumption directly. When the thermal-induced optical power loss is large, the VCSEL power consumption dominates the total power consumption of the O/E interface. Figure 2 shows that O/E power consumption keeps at a relatively low level in low loss range, but increases exponentially when loss is large. In order to avoid significant thermal-induced optical power loss, we propose an initial device setting and thermal-tuning mechanism.

4.2 Initial device setting condition

Thermal tuning of silicon MRs by local microheaters is a solution to compensate for the thermal-induced variation as well as the fabrication error. Tuning efficiency of several mW/nm has been demonstrated in related research works [Gan et al. 2007]. Note that thermal tuning is only able to red-shift the resonant wavelength by heating, but cannot shift the resonant wavelength towards the opposite direction. If the resonant wavelength of MR is smaller than the input optical signal by $\Delta\lambda$,

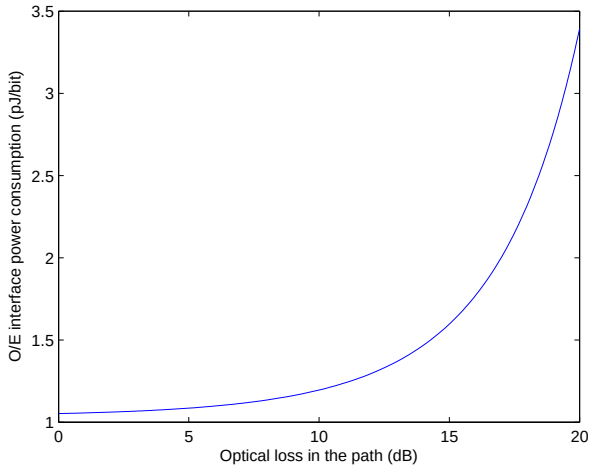

Fig. 2. The impact of optical power loss on O/E power consumption

Table I. Constant Energy Efficiency of O/E Interface

O/E interface component	Energy efficiency in 45nm (pJ/bit)
VCSEL driver	0.1125
Photodetector	0.0003
TIA-LA circuit	0.3375
Serializer	0.16
Deserializer	0.128

it can be red-shifted by $\Delta\lambda$ with thermal tuning to match with the input optical signal. Note that the MR resonance is periodic where the wavelength difference between adjacent resonances is the free spectral range (FSR), which is on the order of several tens of nm. If the resonant wavelength of MR is larger than the input optical signal by $\Delta\lambda$, a much larger thermal tuning distance of $FSR-\Delta\lambda$ is needed in order to match the previous resonance with the input optical signal. In order to avoid significant thermal tuning power consumption, we propose an initial device setting condition, which ensures only a small thermal tuning distance of $\Delta\lambda$ is needed.

For a MR in an intermediate switching stage on path, assume that it is working at temperature T_{MR}, and its resonant wavelength λ_{MR} follows Equation (4). Assume that the laser source at the source node of the path is working at temperature T_{VCSEL}, and the lasing wavelength (λ_{VCSEL}) is as Equation (2). In order to ensure that its resonant wavelength can be always red-shifted by thermal tuning to match with the input optical signal, the initial setting of MR (λ_{MR_0}) at room temperature T_0 should follow Equation (9), where we assume the on-chip temperature varies in the range of $[T_{MIN}, T_{MAX}$.

$$\lambda_{MR\_0} = \lambda_{VCSEL\_0} + \rho_{VCSEL} \cdot (T_{MIN} - T_0) - \rho_{MR} \cdot (T_{MAX} - T_0) \qquad (9)$$

4.3 Thermal tuning distance

With the proposed initial setting, the resonant wavelength of MR working at any $T_{MR}\epsilon[T_{MIN}, T_{MAX}]$ is always smaller than the lasing wavelength of the laser source working at any $T_{VCSEL}\epsilon[T_{MIN}, T_{MAX}]$, thus thermal tuning can be applied to red-shift it until it matches with the optical signal. With the proposed initial setting, the tuning distance is as Equation (10).

$$\Delta\lambda_{tuning} = \rho_{VCSEL} \cdot (T_{VCSEL} - T_{MIN}) + \rho_{MR} \cdot (T_{MAX} - T_{BOSE}) \quad (10)$$

The power consumption for thermal tuning can be estimated as Equation (11), where c is the tuning power efficiency in mW/nm.

$$P_{tuning} = c \cdot \Delta\lambda_{tuning} \quad (11)$$

5. A LEARNING-BASED THERMAL-SENSITIVE ADAPTIVE ROUTING ALGORITHM FOR POWER OPTIMIZATION

On the basis of the initial device setting and thermal tuning mechanism described in the last section, we propose a learning-based thermal-sensitive adaptive routing algorithm to find optimal paths with the minimum estimated thermal-induced power consumption. In this section, we will first briefly introduce the circuit switching mechanism that is adopted in the proposed optical NoC. Then we will describe the details of the proposed learning-based thermal-sensitive adaptive routing algorithm.

5.1 Circuit switching

Circuit switching is adopted in the proposed optical NoC, in which a whole optical path is reserved before payload transmission. An overlapped electronic control network is used for reservation and maintenance of optical paths. For each packet to be sent, the router control unit at the source node generates a single-flit setup packet to be routed in the electronic control network. The routing algorithm decides how the setup packet selects a path. When it passes through an intermediate node, it not only reserves the optical resources on the path, but also reserves the electronic path in the control network. A reservation table is used in each router control unit to identify the state of the local router ports. Deadlock-free is guaranteed by using the odd-even turn model to find feasible paths to be learnt by the proposed learning-based thermal-sensitive adaptive routing algorithm. If the path reservation is successful, an optical acknowledgement signal would be generated by the destination and sent back to the source along the reserved optical path. Upon receiving the acknowledgement, the source processor will pass the payload to local O/E interface. High-speed optical transmission is achieved without buffering in intermediate routers. After payload transmission, the reserved path will be released by routing a tear-down packet along the successfully pre-reserved path in the electronic control network. A quickly acknowledge and simultaneously tear-down protocol is used to reduce control delays of the acknowledgement and tear-down processes [Ye et al. 2013].

5.2 A learning-based thermal-sensitive adaptive routing algorithm

Routing algorithms can be classified as deterministic or adaptive. For mesh or torus-based NoCs, the traditional dimension-order routing (e.g., XY routing) is

a deterministic routing algorithm which always selects a fixed path for the same communication pair. Due to the deterministic feature, it cannot avoid bad paths according to runtime network conditions. Different from deterministic routing, adaptive routing can dynamically make routing decision according to runtime network conditions. The odd-even routing is a deadlock-free adaptive routing algorithm with high routing adaptivity and has been widely used in NoC designs [Chiu 2000]. Besides, Q-routing is an adaptive routing algorithm based on the Q-learning technique [Farahnakian et al. 2011; Ebrahimi et al. 2012]. In Q-routing based NoCs, each node in the network keeps a Q-table which stores Q-values. The Q-values represent the quality or cost (e.g., latency) of alternative paths. Each node learns the state of the network (e.g., network congestion) by receiving Q-values from neighboring nodes, and uses these Q-values to dynamically make routing decisions. Each node updates their Q-table when it receives updated Q-values from its neighboring nodes.

In optical NoCs, on-chip temperature variations cause significant thermal-induced optical power loss and power consumption. In the last section, we proposed an initial device setting and thermal-tuning mechanism to avoid significant thermal-induced optical power loss inserted in switchings. In this section, on the basis of the proposed initial device setting and thermal-tuning mechanism, we propose a learning-based thermal-sensitive adaptive routing algorithm to optimize path selections according to runtime on-chip temperature distributions. Simulation results demonstrated that the proposed learning-based thermal-sensitive adaptive routing algorithm together with the proposed initial device setting and thermal tuning mechanism can improve the power efficiency at little expense of performance overhead.

5.2.1 *E-value.* In traditional Q-routing based electronic NoCs, Q-values represent the latency of alternative paths, and the Q-learning technique is performed to learn network congestions by Q-values. It optimizes the path selections for latency optimization. This work targets optical NoCs in presence of temperature variations, and focuses on the optimization of thermal-induced energy consumption. We use the odd-even turn model to find a set of deadlock-free feasible shortest paths for each source-destination communication pair. The set of alternative paths found are provided to be learnt by the proposed learning-based thermal-sensitive adaptive routing algorithm. We use the Q-learning technique to learn the runtime on-chip temperature information and find optimal paths with the minimum estimated thermal-induced energy consumption.

Each node in the optical NoC keeps an E-table which stores E-values. The E-values represent the estimated thermal-induced energy consumption of alternative paths. Each node learns the state of the network by receiving E-values from neighboring nodes. When a node receives updated E-values from its neighboring nodes, it updates its local E-table. For a packet to be sent from the source node s to the destination node d, assume that its setup packet just went by the node x and is currently at node y (Figure 3). Assume that $N(y)$ is the set of feasible next nodes found by the odd-even routing, we define $E_y(s, n, d)$ as the E-value representing the estimated thermal-induced energy consumption from any feasible next node $n \epsilon N(y)$ to the destination. As shown in Equation (12), the neighboring node

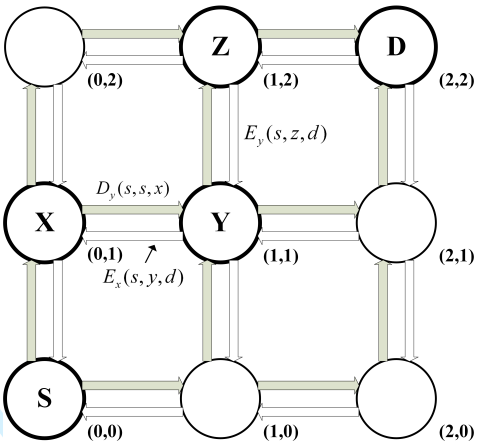

Fig. 3. An example of the proposed learning-based routing in a 3x3 mesh network

$z \epsilon N(y)$ which is with the minimum estimated thermal-induced energy consumption will be selected as the next node.

$$E_y(s,z,d) = \min_{n \epsilon N(y)} E_y(s,n,d) \tag{12}$$

As soon as node y forwards the setup packet to the next node z, node y will send a E-value $E_x(s,y,d)_{est}$ back to its previous node x, which indicates the best estimated thermal-induced energy consumption from the node y to the node d. As shown in Equation (13), $E_x(s,y,d)_{est}$ is equal to the sum of two quantities, where $E_y(s,z,d)$ is the minimum estimated thermal-induced energy consumption from node z to the destination, and e_y is the thermal-induced energy consumed at the node y.

$$E_x(s,y,d)_{est} = E_y(s,z,d) + e_y \tag{13}$$

After receiving the new best estimated E-value $E_x(s,y,d)_{est}$ from the node y, the node x will update its old E-value. The Q-learning is performed by updating the E-value according to Equation (14), where r is the learning rate which determines how fast the newer value overwrites the older one.

$$E_x(s,y,d)_{new} = E_x(s,y,d)_{old} + r\left(E_x(s,y,d)_{est} - E_x(s,y,d)_{old}\right) \tag{14}$$

As described in Section 4, the thermal-induced energy consumption for packet transmission in optical NoC includes the energy consumed by O/E interfaces which is dominated by the thermal-induced optical power loss in path, and the energy consumed for thermal tuning. Correspondingly, the E-value is determined by t-wo quantities, one is the estimated optical power loss from the next node to the destination which decides the energy consumption of O/E interface, and another is the estimated thermal tuning energy consumption from the next node to the destination.

For a packet sent from the source node s, when it passes through an intermediate node i towards the destination, we define $l(s,i)$ as the optical power loss inserted by the node i and $t(s,i)$ as the thermal tuning energy consumed at the node i. $l(s,i)$

and $t(s,i)$ are sensitive to the temperature in the source node s which determines the lasing wavelength, and the temperature in the node i which determines the resonant wavelength of the optical switching element. By adding up the optical power loss inserted by each node in the path, we get the total optical power loss in the path and then we can calculate the energy consumption of the O/E interface. Meanwhile, by adding up the thermal tuning energy consumption in each node in the path, we get the total thermal tuning energy consumption in the path. The total energy consumption for the packet transmission is the sum of the energy consumption of the O/E interface and the total thermal tuning energy consumption.

Assume that node x and node y are two intermediate nodes in the path, we define $L(s,x,y)$ as the optical power loss from node x to node y, and $T(s,x,y)$ as the thermal tuning energy consumption from node x to node y. We divide the estimated optical power loss of the whole path from the source node s to the destination node d into three parts: (1) the optical power loss from the source node s to the node x, $L_y(s,s,x)$, where y is the current node; (2) $l(s,y)$, which is the optical power loss inserted in the node y; (3) $L_y(s,z,d)$, which is the estimated optical power loss from the node z to the destination node d. Similarly, we divide the estimated thermal tuning energy consumption in the whole path into three parts: (1) $T_y(s,s,x)$, which is the thermal tuning energy consumption from the source node s to the node x; (2) $t(s,y)$, which is thermal tuning energy consumption in the node y; (3) $T_y(s,z,d)$, which is the estimated thermal tuning energy consumption from the node z to the destination node d.

We define $D_y(s,s,x)$ as a value representing the energy consumption from the source node s to the node x. $D_y(s,s,x)$ is determined by two quantities, one is the optical power loss $L_y(s,s,x)$, and another is the thermal tuning energy consumption $T_y(s,s,x)$. Different from the E-value, $D_y(s,s,x)$ is inserted in the setup packet and delivered from the node x to the node y with the setup packet. Besides, the E-value $E_y(s,z,d)$ is determined by two quantities, one is the minimum estimated optical loss $L_y(s,z,d)$ from the node z to the destination node d, and another is the minimum estimated thermal tuning energy consumption $T_y(s,z,d)$. As described before, $E_y(s,z,d)$ can be learnt from the E-table.

So when the setup packet is in the node y, it can estimate the total optical power loss $L(s,s,d)$ in the whole path and the total thermal tuning energy consumption $T(s,s,d)$ respectively as Equation (15) and Equation (16), where the N is the set of passing nodes from node s to node d, and y is the current node. With the estimated optical power loss of the whole path, we can get the estimated energy consumption dissipated by O/E conversions. By adding it to the estimated thermal tuning energy consumption, we can get the estimated total energy consumption.

$$L(s,s,d) = \sum_{i \epsilon N} l_i = L_y(s,s,x) + l(s,y) + L_y(s,z,d) \tag{15}$$

$$T(s,s,d) = \sum_{i \epsilon N} T_i = T_y(s,s,x) + t(s,y) + T_y(s,z,d) \tag{16}$$

5.2.2 *E-table.* Table II shows an example of the E-table in node y, with address (1,1) in the 3x3 mesh network (Figure 3). The E-table has three fields: the state-space, the action-space and the E-value field. The state-space stores the address

Table II. An example of E-table

State-Space					Action-Space		E-value E(s,z,d)			
y	s	d	z		a		L(s,z,d)		T(s,z,d)	
Cur	Src	Dest	Next		Output-Port		Optical Loss		Tuning Energy	
(1,1)	(0,0)	(2,1)	(2,1)	-	East	-		-		-
(1,1)	(0,0)	(1,2)	(1,2)	-	Up	-		-		-
(1,1)	(0,0)	(2,2)	(1,2)	(2,1)	Up	East				
(1,1)	(0,1)	(2,1)	(2,1)	-	East	-		-		-
(1,1)	(0,1)	(1,2)	(1,2)	-	Up	-		-		-
(1,1)	(0,1)	(2,2)	(1,2)	(2,1)	Up	East				

information of the current node, the source node, the destination node, and feasible next nodes found by odd-even routing. The action space stores the output ports in the current node towards each feasible next node. In mesh or torus-based optical NoC, the feasible output ports are within the following cases: left, right, up, down and local directions. For example, for a setup packet that is routed from the source node with address (0,0) to the destination node with address (2,2) in the 3x3 mesh network (Figure 3), when the setup packet is currently in the node y with address (1,1), feasible output ports includes the Up output port towards the neighbouring node with address (1,2), and the East output port towards the neighboring node with address (2,1). The E-value field consists of two subfields, one is the estimated optical power loss from the next node to the destination, and another is the estimated thermal tuning energy consumption from the next node to the destination. In the proposed learning-based thermal-sensitive adaptive routing, each node utilizes the E-values to estimate the total thermal-induced energy consumption in alternative path, and then dynamically make routing decisions to find optimal paths with the minimum estimated thermal-induced energy consumption.

5.2.3 *The routing algorithm.* Algorithm 1 presents the procedure of path selection in the proposed learning-based thermal-sensitive adaptive routing. For a setup packet $p(s,d)$ that is routed from the source node s to the destination node d, assume that it is currently at an intermediate node y. The routing unit at the node y first gets a set of valid output ports ($Set_{output-port}$) with the odd-even routing, which guarantees that alternative paths found are shortest and deadlock free. Then the optimal selection function selects an optimal output port from $Set_{output-port}$ with the minimum estimated thermal-induced energy consumption towards the destination node. Algorithm 2 shows how the optimal selection function decides the optimal output port. In detail, if the size of $Set_{output-port}$ is only one, it just returns the only valid output port. If the size of $Set_{output-port}$ is two, it compares the estimated thermal-induced energy consumption according to E-values stored in the E-table, and returns the output port with less estimated thermal-induced energy consumption towards the destination node. After the current node forwards the setup packet $p(s,d)$ to the next node through the selected output port, it sends back a learning packet which contains the E-value to the previous node. Upon

receiving the learning packet, the previous node updates the corresponding E-value in E-table.

Algorithm 1 The proposed learning-based thermal-sensitive adaptive routing algorithm

1: Receive $p(s,d)$ at current node y
2: Get $Set_{output-port}$ with odd-even routing
3: Select an optimal output-port from $Set_{output-port}$ by the Optimal Selection function
4: Send $p(s,d)$ to the next node through the selected optimal output port
5: Send a learning packet back to the previous node
6: Update the E-table after receive the learning packet

Algorithm 2 The Optimal Selection Function

$Dest\_id \leftarrow Get_Dest()$
2: **if** $Dest\_id = local\_router\_id$ **then**
    return the direction to Processor
4: **end if**
if $Size_{Output-Port} = 1$ **then**
6: **return** the Output-Port
end if
8: **if** $Size_{Output-Port} = 2$ **then**
    $Energy\_Neighbor1_{est} \leftarrow E\text{-}table(s,d,Neighbor1)$
10: $Energy\_Neighbor2_{est} \leftarrow E\text{-}table(s,d,Neighbor2)$
    if $Energy\_Neighbor1_{est} <= Energy\_Neighbor2_{est}$ **then**
12: **return** Neighbor1
    else if $Energy\_Neighbor1_{est} > Energy\_Neighbor2_{est}$ **then**
14: **return** Neighbor2
    end if
16: **end if**

6. SIMULATION RESULTS AND COMPARISONS

In order to evaluate the effectiveness of our approach, we developed a SystemC-based cycle-accurate network simulator for an 8x8 mesh-based optical NoC with the proposed learning-based thermal-sensitive adaptive routing. 64 non-blocking 5x5 fully-connected Cygnus optical routers are used to build the 8x8 mesh-based optical NoC [Gu et al. 2009]. Each Cygnus optical router uses 16 MRs to implement a 5x5 switching function. Besides, we use a matched 8x8 mesh-based optical NoC with the traditional XY routing as a baseline for comparison. We assume that both of the proposed optical NoC and the baseline optical NoC adopt the proposed initial device setting and thermal tuning mechanism to compensate for the temperature-dependent wavelength shift. Network simulations are conducted under several random traffic patterns, as well as a set of real applications.

6.1 The convergence of the proposed routing algorithm

In order to show the convergence of the proposed learning-based thermal-sensitive adaptive routing algorithm, we simulate an 8x8 mesh-based optical NoC with the proposed routing algorithm under uniform traffic. A random temperature distribution is applied in the simulation, and we assume that the on-chip temperature is within the range of $[55^oC, 85^oC]$. Figure 4 shows the convergence of energy efficiency optimization for delivering packets from node 0 to node 63, from node 0 to node 47, and from node 0 to node 15. It is shown that for packets belongs to the same source-destination communication pair, the thermal-induced energy consumption for packet transmission varies before the proposed routing algorithm reaches the state of convergence. After learning the network with a certain number of packets, the proposed learning-based routing algorithm reaches the state of convergence, which means that it finds the optimal path with optimized thermal-induced energy consumption. For example, for packets sent from node 0 to node 63, it finds the optimal path after learning more than 80 packets. The optimal path is with energy efficiency of about 22 pJ/bit. For packets sent from node 0 to node 15, it finds the optimal path with energy efficiency of about 14 pJ/bit after learning less than 20 packets. It can be observed that for a longer path, it needs to learn more packets to find the optimal path.

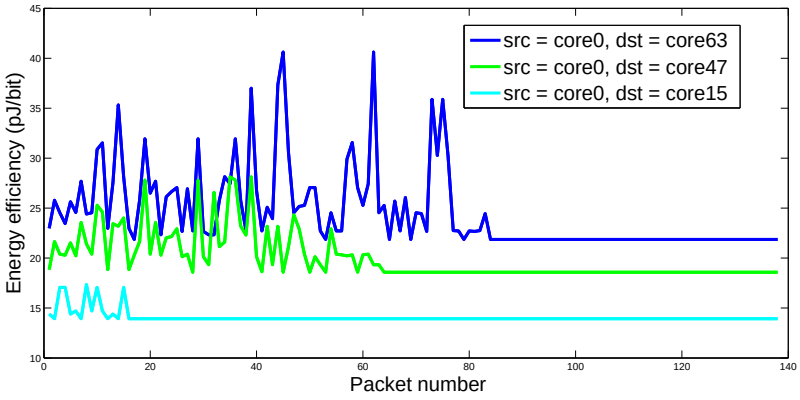

Fig. 4. The convergence of energy efficiency optimization by the proposed learning-based routing

6.2 Thermal-induced energy efficiency

In the following, we present more simulation results and comparisons in terms of thermal-induced energy efficiency, under a set of real applications as well as a set of random traffic patterns.

6.2.1 *Real applications.* We simulate an 8x8 mesh-based optical NoC with the proposed learning-based thermal-sensitive adaptive routing under a set of real applications including FPPPP, H264DH, ROBOT, SAMPLE, SATELL, and SPARSE.

A matched 8x8 mesh-based optical NoC with the traditional XY routing is simulated as a baseline for comparison. In order to show the effectiveness of the proposed learning-based thermal-sensitive adaptive routing algorithm, we assume both of the proposed optical NoC and the baseline optical NoC adopt the proposed initial device setting and thermal tuning mechanism to compensate for the temperature-dependent wavelength shift. For each real application, we use traffic information to simulate the on-chip temperature distribution by HotSpot [Huang et al. 2006] together with McPAT [Li et al. 2009].

Figure 5 shows the worst-case energy efficiency among all packets transmission under each real application. It shows that for the 8x8 mesh-based optical NoC with either the proposed routing or the baseline XY routing, the proposed initial device setting and thermal tuning mechanism confines the worst-case thermal-induced energy consumption to be on the order of tens of pJ/bit. This is because it avoids significant optical power loss caused by the temperature-dependent wavelength shift by thermal tuning, and the thermal tuning distance is limited by the initial device setting. Besides, it is shown that the proposed routing achieves a better worst-case energy efficiency for all the real applications simulated, except for the ROBOT application. Under the ROBOT application, the proposed routing has the same worst-case energy efficiency with the baseline XY routing. On the average of all the six real applications, the proposed routing reduces the worst-case energy consumption by 16.8% than the baseline XY routing algorithm. It can be concluded that for applications with more heavy and long-distance traffic, such as the H264DH and SAMPLE and SATELL, the proposed routing algorithm has a greater space for optimization, and thus it achieves more significant improvements. For example, under the H264DH application, the proposed routing reduces the worst-case energy consumption by 28.0% than the baseline XY routing algorithm. Under the SAMPLE application, the proposed routing reduces the worst-case energy consumption by 31.1% than the baseline XY routing algorithm. Meanwhile, for applications with more short-distance traffic, the space for optimization by the proposed routing is smaller. For example, under the ROBOT application, all the packets transmission are between near source-destination communication pairs, so the worst-case energy efficiency of our proposed routing is almost the same with the baseline XY routing.

Figure 6 shows the average energy efficiency of all packets transmission under each real application. It shows that the proposed routing achieves a better average energy efficiency for all the real applications simulated. On the average of the six real applications, the proposed routing reduces the average energy consumption by 5.1% than the XY routing. Similar conclusions can be got as conclusions from Figure 5. For applications with more long-distance traffic, the proposed routing algorithm has a greater space for optimization, and thus it achieves more significant improvements as compared to the XY routing. For example, under the H264DH application, the proposed routing reduces the average energy consumption by 9.2% than the XY routing.

6.2.2 *Random traffic patterns.* In addition to the set of real applications, we also simulate the 8x8 mesh-based optical NoC with the proposed learning-based thermal sensitive adaptive routing algorithm under a set of random traffic patterns, including BitReverse, Hotspot, Transpose and Uniform. Different from simulations

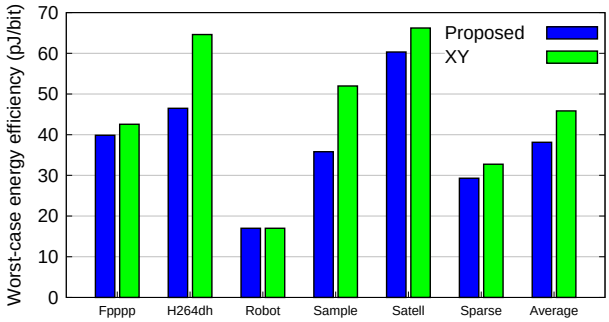

Fig. 5. The worst-case energy efficiency under real applications, with simulated temperature distributions

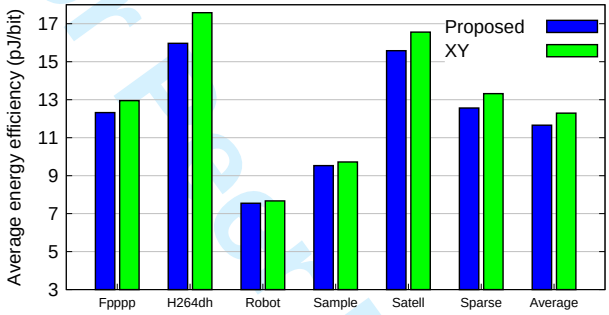

Fig. 6. Average energy efficiency under real applications, with simulated temperature distributions

for the real applications, here we apply random on-chip temperature distributions in the simulations. We assume that the on-chip temperature is within the range of $[55^oC, 85^oC]$.

Figure 7 shows the comparison of the worst-case energy efficiency among all packets transmission under each random traffic pattern. We compare the proposed routing with the baseline XY routing. It shows that for all the four random traffic patterns, the proposed thermal-sensitive routing always has a better worst-case energy efficiency than the XY routing. On average of the four random traffic patterns, it reduces the worst-case energy efficiency by 19.2% as compared to the XY routing. It also shows that the improvement is more obvious when the traffic pattern contains more long-distance traffic. For example, for the BitReverse traffic pattern, the proposed routing improves the worst-case energy efficiency by 33.1% as compared to the XY routing. In contrast, for the Hotspot traffic pattern where most packets are delivered between near communication pairs, the space for optimization by the proposed routing is much smaller.

Figure 8 shows the comparison of the average energy efficiency of all packets under

each random traffic pattern. Similar conclusions can be got as the comparison of the worst-case energy efficiency. It also shows that for all the four random traffic patterns, the proposed thermal-sensitive routing always has a better average energy efficiency than the XY routing. On average of the four random traffic patterns, it reduce the average energy efficiency by 20.8% as compared to the XY routing. It also shows that the improvement is more obvious when the traffic pattern contains more long-distance traffic. For example, for the BitReverse traffic pattern, the proposed routing improves the average energy efficiency by 29.3% as compared to the XY routing.

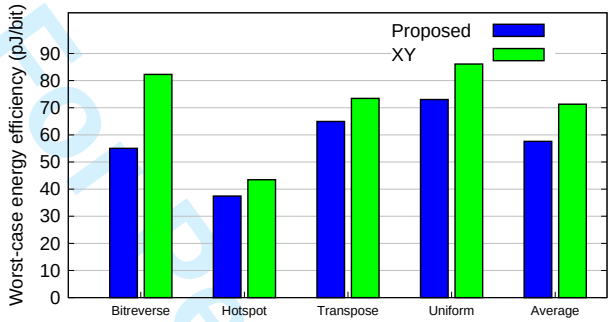

Fig. 7. The worst-case energy efficiency under random traffic patterns, with random temperature distributions

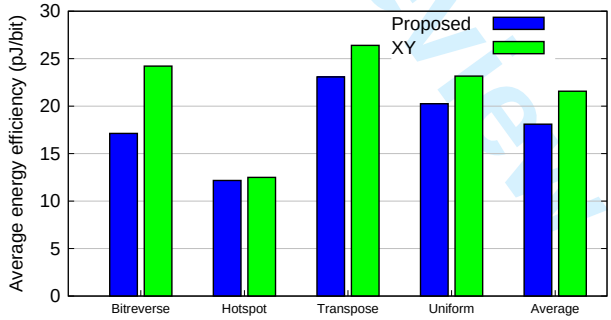

Fig. 8. Average energy efficiency under random traffic patterns, with random temperature distributions

6.3 Network performance

In the proposed learning-based thermal-sensitive adaptive routing, we use odd-even routing to find feasible paths for learning. This guarantees that all the feasible paths found are shortest paths and deadlock free. This ensures that the proposed routing can achieve the power optimization at little expense of network performance sacrifice. In the following, we show the network performance of the 8x8 mesh-based optical NoC with the proposed routing under the set of real applications as well as the set of random traffic patterns.

Figure 9 shows the comparison of normalized network performance under each real application. Here the network performance is measured in terms of the total number of execution times of an application within a fixed number of clock cycles. It is shown that the network performance with the proposed routing is very close to the baseline optical NoC with the XY routing. On average of the six real applications, the network performance decreases by 4% than the traditional XY routing.

Figure 10 shows the normalized network throughput of the 8x8 mesh-based optical NoC with the proposed routing under each random traffic pattern, where the injection rate is set as 0.1. It shows that for traffic patterns with more long-distance traffic, such as the BitReverse traffic pattern, the proposed routing achieves almost the same network throughput as the XY routing. In contrast, for traffic patterns where most of traffics are short-distance, such as the Hotspot, the XY routing outperforms the proposed routing. It can be concluded that, the proposed routing algorithm works better for applications with heavy and long-distance traffic.

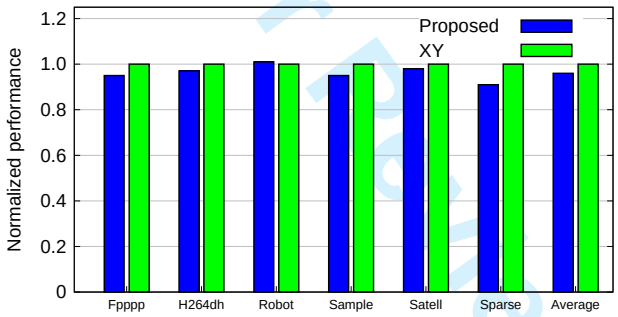

Fig. 9. Normalized performance under different real applications

7. CONCLUSIONS

In this work, we proposed a learning-based thermal-sensitive power optimization approach for mesh or torus-based optical NoCs in presence of temperature variations. The key techniques proposed includes an initial device setting and thermal tuning mechanism which is a device-level optimization technique, and a learning-based thermal-sensitive adaptive routing algorithm which is a network-level optimization

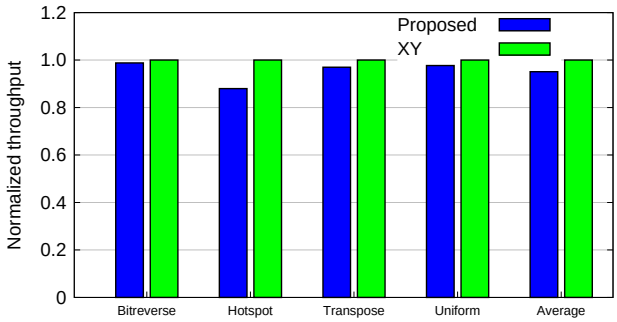

Fig. 10. Normalized throughput under different random traffic patterns

technique. Simulation results of an 8x8 mesh-based optical NoC show that the proposed initial device setting and thermal tuning mechanism confines the worst-case thermal-induced energy consumption to be on the order of tens of pJ/bit. Besides, the learning-based thermal-sensitive adaptive routing algorithm is proposed to find optimal paths with the minimum estimated thermal-induced power consumption for packet transmission. Simulation results show that the proposed learning-based thermal-sensitive adaptive routing algorithm can find an optimal path for each communication pair by learning the network state after delivering a certain number of packets. The proposed routing has a greater space for optimization especially for applications with more long-distance traffic.

REFERENCES

Asadi, B., Reshadi, M., and Khademzadeh, A. 2016. A routing algorithm for reducing optical loss in photonic networks-on-chip. *Photonic Network Communications*.

Baehr-Jones, T., Hochberg, M., Walker, C., Chan, E., Koshinz, D., Krug, W., and Scherer, A. 2005. Analysis of the tuning sensitivity of silicon-on-insulator optical ring resonators. *J. Lightwave Technology 23,* 12, 4215–4221.

Benini, L. and De Micheli, G. 2002. Networks on chip: a new paradigm for systems on chip design. In *Proc. Design, Automation and Test in Europe Conference and Exhibition*. 418–419.

Chen, C., Leisher, P., Allerman, A., Geib, K., and Choquette, K. 2006. Temperature analysis of threshold current in infrared vertical-cavity surface-emitting lasers. *IEEE J. Quantum Electronics 42,* 10, 1078–1083.

Chiu, G.-M. 2000. The odd-even turn model for adaptive routing. *IEEE Transactions on Parallel and Distributed Systems 11,* 7, 729–738.

Dally, W. and Towles, B. 2001. Route packets, not wires: on-chip interconnection networks. In *Proc. Design Automation Conf.* 684–689.

Della Corte, F. G., Esposito Montefusco, M., Moretti, L., Rendina, I., and Cocorullo, G. 2000. Temperature dependence analysis of the thermo-optic effect in silicon by single and double oscillator models. *J. Applied Physics 88,* 12, 7115–7119.

Dokania, R. K. and Apsel, A. B. 2009. Analysis of challenges for on-chip optical interconnects. In *Proc. 19th ACM Great Lakes Symp. VLSI*. 275–280.

Dumon, P., Priem, G., Nunes, L., Bogaerts, W., Van Thourhout, D., Bienstman, P., Liang, T., Tsuchiya, M., Jaenen, P., Beckx, S., Wouters, J., and Baets, R. 2006. Linear and nonlinear nanophotonic devices based on silicon-on-insulator wire waveguides. *Japanese J. Applied Physics*, 6589–6602.

Ebrahimi, M., Daneshtalab, M., Farahnakian, F., Plosila, J., Liljeberg, P., Palesi, M., and Tenhunen, H. 2012. Haraq: Congestion-aware learning model for highly adaptive routing algorithm in on-chip networks. In *2012 IEEE/ACM Sixth International Symposium on Networks-on-Chip*. 19–26.

Farahnakian, F., Ebrahimi, M., Daneshtalab, M., Liljeberg, P., and Plosila, J. 2011. Q-learning based congestion-aware routing algorithm for on-chip network. In *2011 IEEE 2nd International Conference on Networked Embedded Systems for Enterprise Applications*. 1–7.

Faralli, S., Andriolli, N., Gambini, F., Pintus, P., Preve, G., Chiesa, M., Ortu?o, R., Liboiron-Ladouceur, O., and Cerutti, I. 2016. Bidirectional transmissions in a ring-based packaged optical noc with 12 add-drop microrings. In *2016 IEEE Photonics Conference (IPC)*. 621–622.

Feng, C., Lu, Z., Jantsch, A., Li, J., and Zhang, M. 2010. A reconfigurable fault-tolerant deflection routing algorithm based on reinforcement learning for network-on-chip. In *Proceedings of the Third International Workshop on Network on Chip Architectures*. NoCArc '10. ACM, New York, NY, USA, 11–16.

Gan, F., Barwicz, T., Popovic, M., Dahlem, M., Holzwarth, C., Rakich, P., Smith, H., Ippen, E., and Kartner, F. 2007. Maximizing the thermo-optic tuning range of silicon photonic structures. In *Photonics in Switching*. 67–68.

Geng, M., Jia, L., Zhang, L., Yang, L., Chen, P., Wang, T., and Liu, Y. 2009. Four-channel reconfigurable optical add-drop multiplexer based on photonic wire waveguide. *Opt. Express 17,* 7, 5502–5516.

Gu, H., Mo, K. H., Xu, J., and Zhang, W. 2009. A low-power low-cost optical router for optical networks-on-chip in multiprocessor systems-on-chip. In *IEEE Computer Society Annual Symp. VLSI*. 19–24.

Guo, P., Hou, W., Guo, L., Cai, Q., Zong, Y., and Huang, D. 2015. Reliable routing in 3d optical network-on-chip based on fault node reuse. In *2015 7th International Workshop on Reliable Networks Design and Modeling (RNDM)*. 92–98.

Huang, W., Ghosh, S., Velusamy, S., Sankaranarayanan, K., Skadron, K., and Stan, M. R. 2006. Hotspot: a compact thermal modeling methodology for early-stage vlsi design. *IEEE Transactions on Very Large Scale Integration (VLSI) Systems 14,* 5, 501–513.

Ji, R., Yang, L., Zhang, L., Tian, Y., Ding, J., Chen, H., Lu, Y., Zhou, P., and Zhu, W. 2011. Five-port optical router for photonic networks-on-chip. *Opt. Express 19,* 21, 20258–20268.

Koester, S., Schares, L., Schow, C., Dehlinger, G., and John, R. 2006. Temperature-dependent analysis of Ge-on-SOI photodetectors and receivers. In *3rd IEEE Int. Conf. Group IV Photonics*. 179–181.

Kromer, C., Sialm, G., Berger, C., Morf, T., Schmatz, M., Ellinger, F., Erni, D., Bona, G.-L., and Jackel, H. 2005. A 100-mW 4 x 10 Gb/s transceiver in 80-nm CMOS for high-density optical interconnects. *IEEE J. Solid-State Circuits 40,* 12, 2667–2679.

Lee, J.-M., Kim, D.-J., Ahn, H., Park, S.-H., and Kim, G. 2007. Temperature dependence of silicon nanophotonic ring resonator with a polymeric overlayer. *J. Lightwave Technol. 25,* 8, 2236–2243.

Li, H., Fourmigue, A., Beux, S. L., Letartre, X., O'Connor, I., and Nicolescu, G. 2015a. Thermal aware design method for vcsel-based on-chip optical interconnect. In *2015 Design, Automation Test in Europe Conference Exhibition (DATE)*. 1120–1125.

Li, S., Ahn, J. H., Strong, R. D., Brockman, J. B., Tullsen, D. M., and Jouppi, N. P. 2009. Mcpat: An integrated power, area, and timing modeling framework for multicore and manycore architectures. In *2009 42nd Annual IEEE/ACM International Symposium on Microarchitecture (MICRO)*. 469–480.

Li, Z., Mohamed, M., Chen, X., Dudley, E., Meng, K., Shang, L., Mickelson, A. R., Joseph, R., Vachharajani, M., Schwartz, B., and Sun, Y. 2010. Reliability modeling and management of nanophotonic on-chip networks. *Very Large Scale Integration (VLSI) Systems, IEEE Transactions on PP,* 99, 1–14.

Li, Z., Qouneh, A., Joshi, M., Zhang, W., Fu, X., and Li, T. 2015b. Aurora: A cross-layer

solution for thermally resilient photonic network-on-chip. *IEEE Transactions on Very Large Scale Integration (VLSI) Systems 23,* 1, 170–183.

Michalzik, R. and Ebeling, K. J. Operating principles of VCSELs. *University of Ulm, Optoelectronics Department, Germany*.

Mo, K. H., Ye, Y., Wu, X., Zhang, W., Liu, W., and Xu, J. 2010. A hierarchical hybrid optical-electronic network-on-chip. In *IEEE Computer Society Annual Symp. VLSI*. 327–332.

Mogg, S., Chitica, N., Christiansson, U., Schatz, R., Sundgren, P., Asplund, C., and Hammar, M. 2004. Temperature sensitivity of the threshold current of long-wavelength InGaAs-GaAs VCSELs with large gain-cavity detuning. *IEEE J. Quantum Electronics 40,* 5, 453–462.

Morse, M., Dosunmu, O., Sarid, G., and Chetrit, Y. 2006. Performance of Ge-on-Si p-i-n photodetectors for standard receiver modules. *IEEE Photonics Technology Letters 18,* 23, 2442–2444.

Padgaonkar, V. and Arbor, A. 2004. Thermal effects in silicon based resonant cavity devices. *NNIN REU Research Accomplishments*.

Pan, Y., Kumar, P., Kim, J., Memik, G., Zhang, Y., and Choudhary, A. 2009. Firefly: Illuminating future network-on-chip with nanophotonics. In *Proc. 36th Int. Symp. Computer Architecture (ISCA)*.

Poon, A., Luo, X., Xu, F., and Chen, H. 2009. Cascaded microresonator-based matrix switch for silicon on-chip optical interconnection. *Proceedings of the IEEE 97,* 7, 1216–1238.

Poulton, J., Palmer, R., Fuller, A., Greer, T., Eyles, J., Dally, W., and Horowitz, M. 2007. A 14-mW 6.25-Gb/s transceiver in 90-nm CMOS. *IEEE J. Solid-State Circuits 42,* 12, 2745–2757.

Raghunathan, V., Hu, J., Ye, W. N., Michel, J., and Kimerling, L. C. 2010. Athermal silicon ring resonators. In Integrated Photonics Research, Silicon and Nanophotonics. *Integrated Photonics Research, Silicon and Nanophotonics*, IMC5.

Ramini, L., Ghiribaldi, A., Grani, P., Bartolini, S., Fankem, H. T., and Bertozzi, D. 2014. Assessing the energy break-even point between an optical noc architecture and an aggressive electronic baseline. In *2014 Design, Automation Test in Europe Conference Exhibition (DATE)*. 1–6.

Shacham, A., Bergman, K., and Carloni, L. 2007. On the design of a photonic network-on-chip. In *First Int. Symp. Networks-on-Chip*. 53–64.

Skadron, K., Stan, M. R., Sankaranarayanan, K., Huang, W., Velusamy, S., and Tarjan, D. 2004. Temperature-aware microarchitecture: Modeling and implementation. *ACM Trans. Archit. Code Optim. 1,* 1, 94–125.

Syrbu, A., Mereuta, A., Iakovlev, V., Caliman, A., Royo, P., and Kapon, E. 2008. 10 Gbps VCSELs with high single mode output in 1310nm and 1550 nm wavelength bands. In *Conf. Optical Fiber communication/National Fiber Optic Engineers*. 1–3.

Vantrease, D., Schreiber, R., Monchiero, M., McLaren, M., Jouppi, N. P., Fiorentino, M., Davis, A., Binkert, N., Beausoleil, R. G., and Ahn, J. H. 2008. Corona: System implications of emerging nanophotonic technology. In *2008 International Symposium on Computer Architecture*. 153–164.

Werner, S., Navaridas, J., and Lujn, M. 2015. Amon: An advanced mesh-like optical noc. In *2015 IEEE 23rd Annual Symposium on High-Performance Interconnects*. 52–59.

Xiang, D., Zhang, Y., Shan, S., and Xu, Y. 2013. A fault-tolerant routing algorithm design for on-chip optical networks. In *2013 IEEE 32nd International Symposium on Reliable Distributed Systems*. 1–9.

Xiao, S., Khan, M. H., Shen, H., and Qi, M. 2007. Compact silicon microring resonators with ultra-low propagation loss in the C band. *Opt. Express 15,* 22, 14467–14475.

Xie, Y., Nikdast, M., Xu, J., Zhang, W., Li, Q., Wu, X., Ye, Y., Wang, X., and Liu, W. 2010. Crosstalk noise and bit error rate analysis for optical network-on-chip. In *ACM/IEEE Design Automation Conf.* 657–660.

Yang, M. and Ampadu, P. 2016. Thermal-aware adaptive fault-tolerant routing for hybrid photonic-electronic noc. In *Proceedings of the 9th International Workshop on Network on Chip Architectures*. NoCArc'16. ACM, New York, NY, USA, 33–38.

Ye, Y., Wang, Z., Yang, P., Xu, J., Wu, X., Wang, X., Nikdast, M., Wang, Z., and Duong, L. H. K. 2014. System-level modeling and analysis of thermal effects in wdm-based optical networks-on-chip. *IEEE Transactions on Computer-Aided Design of Integrated Circuits and Systems 33,* 11, 1718–1731.

Ye, Y., Xu, J., Huang, B., Wu, X., Zhang, W., Wang, X., Nikdast, M., Wang, Z., Liu, W., and Wang, Z. 2013. 3-d mesh-based optical network-on-chip for multiprocessor system-on-chip. *IEEE Transactions on Computer-Aided Design of Integrated Circuits and Systems 32,* 4, 584–596.

Ye, Y., Xu, J., Wu, X., Zhang, W., Wang, X., Nikdast, M., Wang, Z., and Liu, W. 2012. System-level modeling and analysis of thermal effects in optical networks-on-chip. *Very Large Scale Integration (VLSI) Systems, IEEE Transactions on PP,* 99, 1–14.

Zhang, T., Abelln, J. L., Joshi, A., and Coskun, A. K. 2014. Thermal management of manycore systems with silicon-photonic networks. In *2014 Design, Automation Test in Europe Conference Exhibition (DATE)*. 1–6.

October 2010January 2011May 2011